

MASTER

METAL HYDRIDE SOLAR HEAT PUMP AND POWER SYSTEM (HYCSOS)

by

Richard Gorman and Pamela S. Moritz

NOTICE

This report was prepared as an account of work sponsored by the United States Government. Neither the United States nor the United States Department of Energy, nor any of their employees, nor any of their contractors, subcontractors, or their employees, makes any warranty, express or implied, or assumes any legal liability or responsibility for the accuracy, completeness or usefulness of any information, apparatus, product or process disclosed, or represents that its use would not infringe privately owned rights.

Prepared for

AIAA Conference on
Solar Energy

Phoenix, Arizona

November 27-29, 1978

DISTRIBUTION OF THIS DOCUMENT IS UNLIMITED



U of C-AUA-USDOE

ARGONNE NATIONAL LABORATORY, ARGONNE, ILLINOIS

Operated under Contract W-31-109-Eng-38 for the
U. S. DEPARTMENT OF ENERGY

DISCLAIMER

This report was prepared as an account of work sponsored by an agency of the United States Government. Neither the United States Government nor any agency Thereof, nor any of their employees, makes any warranty, express or implied, or assumes any legal liability or responsibility for the accuracy, completeness, or usefulness of any information, apparatus, product, or process disclosed, or represents that its use would not infringe privately owned rights. Reference herein to any specific commercial product, process, or service by trade name, trademark, manufacturer, or otherwise does not necessarily constitute or imply its endorsement, recommendation, or favoring by the United States Government or any agency thereof. The views and opinions of authors expressed herein do not necessarily state or reflect those of the United States Government or any agency thereof.

DISCLAIMER

Portions of this document may be illegible in electronic image products. Images are produced from the best available original document.

The facilities of Argonne National Laboratory are owned by the United States Government. Under the terms of a contract (W-31-109-Eng-38) between the U. S. Department of Energy, Argonne Universities Association and The University of Chicago, the University employs the staff and operates the Laboratory in accordance with policies and programs formulated, approved and reviewed by the Association.

MEMBERS OF ARGONNE UNIVERSITIES ASSOCIATION

The University of Arizona	Kansas State University	The Ohio State University
Carnegie-Mellon University	The University of Kansas	Ohio University
Case Western Reserve University	Loyola University	The Pennsylvania State University
The University of Chicago	Marquette University	Purdue University
University of Cincinnati	Michigan State University	Saint Louis University
Illinois Institute of Technology	The University of Michigan	Southern Illinois University
University of Illinois	University of Minnesota	The University of Texas at Austin
Indiana University	University of Missouri	Washington University
Iowa State University	Northwestern University	Wayne State University
The University of Iowa	University of Notre Dame	The University of Wisconsin

NOTICE

This report was prepared as an account of work sponsored by the United States Government. Neither the United States nor the United States Department of Energy, nor any of their employees, nor any of their contractors, subcontractors, or their employees, makes any warranty, express or implied, or assumes any legal liability or responsibility for the accuracy, completeness or usefulness of any information, apparatus, product or process disclosed, or represents that its use would not infringe privately-owned rights. Mention of commercial products, their manufacturers, or their suppliers in this publication does not imply or connote approval or disapproval of the product by Argonne National Laboratory or the U. S. Department of Energy.

METAL HYDRIDE SOLAR HEAT PUMP AND POWER SYSTEM (HYCSOS)

Dr. Richard Gorman, P.E., and
Ms. Pamela S. Moritz
TRW Energy Systems Division
7600 Colshire Drive
McLean, Virginia 22101

Abstract

This report presents the design, performance and cost of a solar-powered metal hydride heat pump and power system for use on a residence. This system was first conceived of and its feasibility demonstrated by Dieter Gruen, et. al., at Argonne National Laboratory. The system design, which is limited by heat transfer, was optimized via an iterative computer program. The design process starts with optimizing the thermal transport properties of the hydride-bed-heat exchanger, then traces temperatures and pressures through the operating cycles. The coefficient of performance (COP) of the overall system is then determined from the thermal losses due to cycling the hydride beds and due to the auxiliary power consumed by freon pumps and air-moving fans. The system, using high temperature solar collector input at 210°F to 280°F, provides heating with a COP of approximately 1.6 and cooling with a COP of approximately 0.6, and electrical power during spring and fall, all for a cost comparable to a solar absorption cooler.

I. Introduction

The use of solar energy for building heating and cooling has been a target for the past decade. The available technology (absorption and rankine cycle powered vapor compression refrigeration) have had low coefficients of performance (COP), and thus large solar collector sizes. These large solar collectors are then inactive for most of the spring and fall when heating and cooling are not needed.

The Hydride Conversion and Storage System (HYCSOS) provides heating, cooling and electrical power from solar energy or other low quality input heat. It would thus provide electrical, heat, and air-conditioning output from the solar collectors on a year-round basis. The cost for a HYCSOS which can do all these functions is the same or less than for a solar driven absorption unit of the same cooling capacity.

This investigation's aims are: designing a residential HYCSOS system, evaluating the performance of that design, and establishing the cost of that design. Previous investigations have established HYCSOS feasibility in the 100 ton size.

II. Theoretical Operation

The property of metal hydrides that is utilized for heat pump operation is that, at a given temperature and near constant pressures, metal alloys such as $\text{LaNi}_5\text{-Al}$, and CaNi_5 absorb hydrogen with the release of substantial amounts of heat. With heat input the process is reversible.

Figure 1² shows the characteristic pressure composition curve for $\text{LaNi}_{4.6}\text{Al}_{0.4}\text{H}$ at different temperatures. The use of the two dissimilar metal alloy systems which possess different hydriding isotherms enables one to pump heat from a lower to an intermediate temperature with heat supplied from a higher temperature.

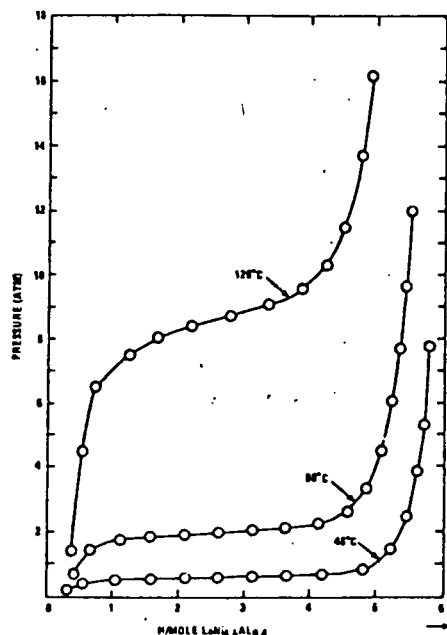


Fig. 1. Dissociation Pressure of $\text{LaNi}_{4.6}\text{Al}_{0.4}\text{H}$

In its simplest form a hydride heat pump would consist of two hydride beds (each containing a different hydride) interconnected to allow hydrogen gas to flow between them. Means would be provided for the input of high temperature heat (from solar concentrating collectors); for heat rejection to or heat acquisition from the atmosphere; and for heat input to or heat rejection from the building. The heat pumping action of the system involves a four-step process. Figures 2 and 3 illustrate the theoretical process which is described below.

In the first step of the process, high temperature (solar) heat is applied to the first bed causing it to desorb hydrogen at high pressure. Because of the pressure differential between the beds, the hydrogen flows to the second bed which is at an intermediate temperature. The hydrogen is absorbed by the second bed with a release of

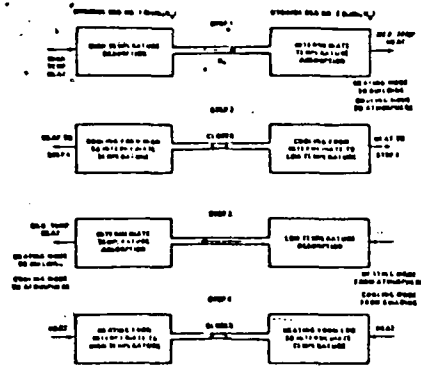


Fig. 2. Block Diagram of Theoretical Hydride Heat Pump Operation.

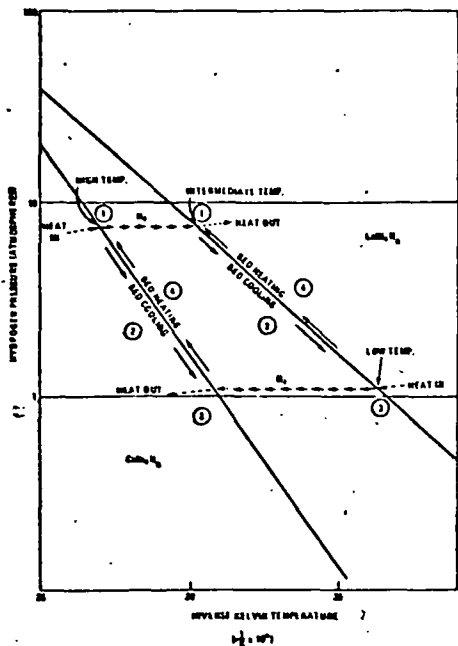


Fig. 3. Theoretical Hydride Heat Pump Cycle.

medium temperature heat. In order to keep the second bed constant at the intermediate temperature, the released heat is rejected to the building (heating mode) or to the atmosphere (cooling mode).

During the second step the hydrogen interconnect is closed, and the two beds are cooled, the first bed to an intermediate temperature and

the second bed to a low temperature. This step is necessary for the correct pressure differential to exist between the beds for reverse hydrogen and heat flow during the next step.

The hydrogen interconnect is opened again during the third step. Heat from the building (cooling mode) or from the atmosphere (heating mode) causes the second bed to desorb hydrogen at a pressure sufficient to cause it to flow to the first bed which is now at an intermediate temperature. The hydrogen is absorbed by the first bed with the release of medium temperature heat. To keep the first bed constant at the intermediate temperature, the released heat is rejected to the building (heating mode) or to the atmosphere (cooling mode).

At this point the hydrogen interconnect is closed and Step Four begins. During this step both beds are heated--the first bed to a high temperature and the second bed to an intermediate temperature--in preparation for the start of the next four-step cycle.

It should be noted that the coefficient of performance (COP) of this theoretical cycle is 1.0 for cooling (2.0 for heating) if the net energy to heat and cool the beds (Steps 2 and 4) is zero. In other words, the heat added to the first bed at high temperature (Step 1) is equal to the heat added to the second bed at lower temperature (Step 3) and the sum is rejected to the atmosphere at the intermediate temperature (Steps 1 and 3).

The beds must be brought from one temperature to another. The energy to heat and cool the beds, while less than the hydriding energy, decreases the COP. The thermal losses are proportional to the temperature swing of the hydride beds and to the total "thermal mass" of the hydrides and their associated heat transfer mechanisms. The lower the "thermal mass" the higher the performance.

To provide a near-continuous heat pumping action the HYCSOS concept uses four hydride beds, two with LaNi_5H_x and two with CaNi_5H_x or $\text{LaNi}_5\text{Al}_3\text{H}_x$. Thus, the respective beds can exchange heat during the temperature change periods (Steps 2 and 4), and with the exception of these periods the heat pumping action is continuous.

The slope of the pressure-composition line for the hydride materials as shown in Figure 1 means that for the hydrogen to be driven out of one hydride bed to the other hydride bed at the end of a desorption-absorption period, the desorbing bed must produce hydrogen at a pressure which is higher than the highest hydrogen pressure for the receiving alloy on the "plateau" of its pressure-composition curve. But the hydrogen from the desorbing bed is at the lowest pressure of its "plateau" on its pressure-composition curve.

This requires higher desorption temperatures than the simple relationship of Figure 3. The single solid lines of Figure 3 become double line: the absorbing pressure versus temperature and the desorbing pressure versus temperature. The absorbing pressure is higher than the desorbing

pressure at a given temperature, causing greater temperature swings in operation and lower efficiency (COP).

The alloy composition $\text{LaNi}_5 \cdot \text{Al}_3$ (for the high temperature bed) is varied in order to optimize the performance of the system at various design temperatures.

The operation of the hydride power cycle is shown in Figures 4 and 5. Only the two high temperature (CaNi_5H_n) beds are cycled.

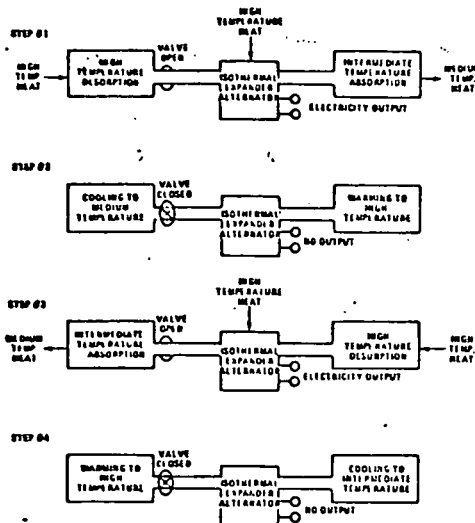


Fig. 4. Theoretical Hydride Power Cycle Operation

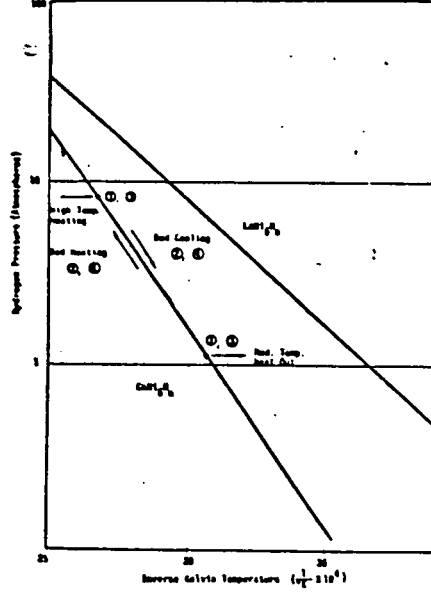


Fig. 5. Electrical Power Generation Cycle

The power generation cycle starts with the high temperature. The addition of heat and the opening of the expander flow valve initiate the power cycle. The hot hydrogen at high pressure (about 10 atmospheres) is expanded isothermally by the addition of heat to the expander during expansion. This additional heat is much less than the desorption energy (about 1100 Btu/lb H_2 compared to 6400 Btu/lb H_2 desorbed). The theoretical efficiency for the isothermal expansion (work out divided by desorption and isothermalization energy) is 0.15. This is comparable to the output of other power cycles working between 250°F and 95°F.

The expanded hydrogen is absorbed by the second CaNi_5H_n bed which is held at the medium temperature by the removal of heat. After the high temperature bed has desorbed all of its hydrogen, the high temperature bed is cooled to the medium temperature and the medium temperature bed (now saturated with hydrogen) is warmed to the high temperature. This is Step 2 in Figure 4. The hydrogen is not allowed to leave the bed while it is being heated. The hydrogen-saturated bed is then desorbed in Step 3 by the addition of heat just as in Step 1. Step 4 is a repeat of Step 2.

III. System Design

The concept for the HYCSOS system is to use a set of four hydride beds. The heat transfer into the beds, and between the HYCSOS beds and the outdoor air heat exchanger, the indoor air heat exchanger, and the solar heat input is provided by condensing and evaporating freon loops. The HYCSOS beds generate high pressure hydrogen which can be expanded through an expander-alternator to produce electricity when not needed for heat or cooling via a heat pump action. Figure 6 shows a schematic of the HYCSOS system analyzed in the heating and cooling modes.

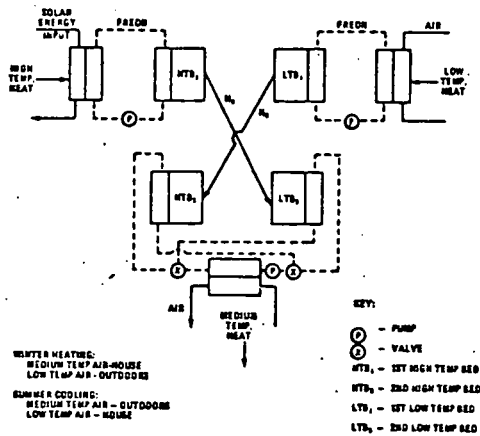


Fig. 6. Hydride Heat Pump or Cooling Cycle

Due to the high cost of the hydride materials (5-7 \$/lb) it is necessary for the hydride beds to cycle very rapidly and frequently in order to maximize the output per unit hydride weight. To facilitate rapid cycling the hydride beds were designed to maximize heat transfer while minimizing hydrogen pressure drop and preventing migration of the hydride particles. Figures 7, 8 and 9 illustrate the design.

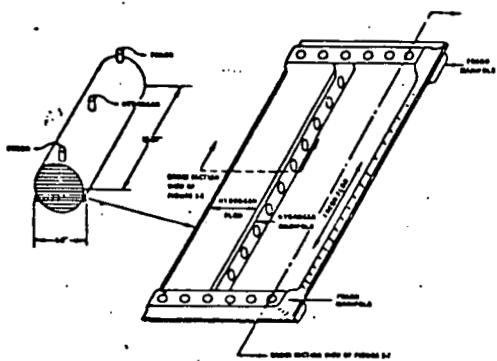


Fig. 7. Hydride Bed Heat Exchanger Assembly and Single Layer.

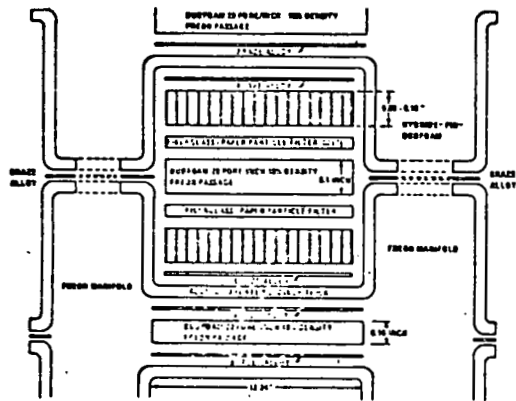


Fig. 8. Hydride Bed Heat Exchanger Cross-Section

The hydride is imbedded in open-pore aluminum foam called Duocel.³ Duocel is made of high thermal conductivity aluminum. The conductivity of Duocel of 5% density, i.e.: 95% void, is about 2.5% of that of high purity aluminum solid material. This is due to the meandering nature of the thermal path in the network of aluminum stands and due to the somewhat lower bulk conductivity of the 6061 alloy from which the Duocel is made. In order to augment the thermal conductivity into the hydride from the freon passages, fins are formed integral with the Duocel perpendicular to the freon passages. The fins are spaced 15 to the inch. The density of the foam between the fins as well as fin thickness can be varied in order to maximize the

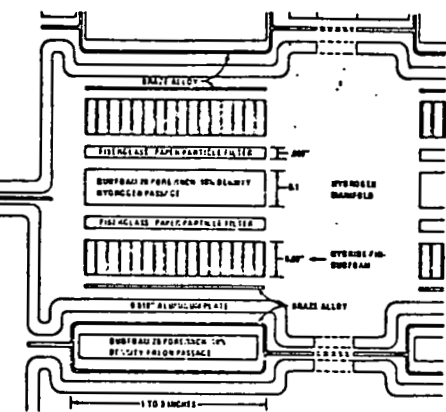


Fig. 9. Hydride Bed Heat Exchanger Cross-Section

the thermal conduction from the freon to the hydride while minimizing the mass of aluminum.

Duocel is also used for the hydrogen and freon passages due to its structural rigidity and high heat transfer properties. The bed is a layered assembly of repeating elements, Figures 8 and 9 showing details of one repeating element from two views at right angles to each other. Fiberglass paper filters are used to prevent carry over of the small hydride flakes.

The number of repeating elements in a specific design is fixed by the rated capacity of the system and by the heat transfer characteristics of a given repeating-element design. Primary sealing is accomplished by brazing of the various manifolds and repeating elements. A secondary hydrogen seal and structural support which restrains the internal pressure forces for the array of repeating elements is provided by enclosing the assembly in a fitted, lightweight, aluminum cylinder. This assembly requires tapering of the stack of repeating elements to conform to the cross-section of the containment cylinder. A typical design results in a complete bed assembly which is a right cylinder, four to six inches in diameter, and one to two feet in length. As may be seen in Figure 7, freon heat-transfer fluid flows through the array in the direction of the axis of the cylinder. Hydrogen flows perpendicular to the axis.

Other system components include valves, pumps and air-freon heat exchangers. The valve subsystem must direct the various flows of freon and hydrogen during cycling and mode changes. The cycling control must provide for two interchanged absorption-desorption cycles and for regeneration between each cycle. The mode changing controls must provide for heating and air-conditioning with heat pump action, heating using direct solar input, power generation with heating, and power generation with outdoor heat rejection. The freon pumps consist of five small centrifugal pumps on a single shaft driven by one motor. The overall freon system is shown in Figure 10. The indoor and outdoor

loops use freon-air heat exchangers of the Duocel type described in Reference 3.

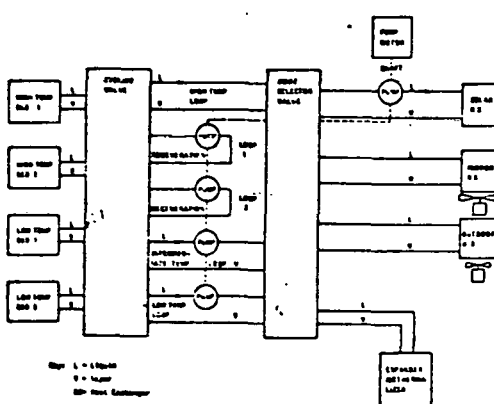


Fig. 10. Overall Freon Schematic

The expander is an isothermal free-piston, double-acting type where the piston forms an element of a reciprocating alternator. The valves are timed by the position and velocity of the piston. The expander operates as a result of the pressure difference between similar hydride beds operated at different temperatures. For HYCSOS the low temperature is either the indoor temperature (when heating is required) or outdoor ambient.

A computer program was developed to assist in the design process. The design heat transfer rate, the aluminum foam and fin thermal conductivity augmentation of the hydride, the outside air temperature drop, and the aluminum doping of the hydride material were all varied to optimize the cost and performance (COP) of the HYCSOS system. The system was optimized for six design temperatures (temperatures for rated winter heat pump operation). Tables 1 and 2⁴ shows the result of the design program process for three sizes of HYCSOS with electrical power generation and for the range of design temperatures.

Table 1. HYCSOS Component Sizing and Power Consumption

WINTER DESIGN TEMP (°F)	DESIGN HEAT OUTPUT (BTU/H)	BED AREA		HYDRIDE MASS		HEAT AREA		FAN POWER		PUMP POWER (WATTS)
		LTD (FT ²)	HTD (FT ²)	INDOOR (LB)	OUTDOOR (LB)	INDOOR (FT ²)	OUTDOOR (FT ²)	INDOOR (WATTS)	OUTDOOR (WATTS)	
25	184	1.56	2.55	241	25	4.6	223	122	77	145
	457	3.95	6.41	641	62	10.0	421	240	145	
	295*	7.81	12.62	16.91	17.8	21.0	16.2	8.5	322	
30	184	1.21	2.01	342	2.5	4.5	223	125	76	145
	457	2.64	4.42	642	6.2	12.5	222	225	240	
	300**	6.83	12.54	16.34	12.4	22.1	15.3	10.5	377	
35	184	1.13	2.03	342	2.5	4.6	223	142	76	145
	457	2.79	6.52	647	6.2	11.6	226	321	105	
	300**	6.43	12.70	16.50	12.2	22.6	15.6	6.7	322	
40	184	1.21	2.04	341	2.8	4.7	223	142	75	145
	457	2.43	5.94	624	6.2	11.6	224	250	105	
	300**	4.61	12.16	15.34	12.1	22.6	15.9	6.7	377	
45	124	1.81	2.91	421	2.5	4.6	223	252	55	145
	457	6.73	7.82	1042	6.2	20.6	624	625	137	
	300**	8.84	12.70	15.95	11.2	27.6	14.0	11.0	247	
47	184	2.01	4.21	626	2.5	6.2	223	152	55	145
	457	4.91	10.41	15.50	6.9	19.7	625	671	137	
	300**	8.97	12.70	15.79	10.0	27.8	14.2	8.3	302	

LTD = LOW TEMPERATURE BED

HTD = HIGH TEMPERATURE BED

*CILING OUTPUT

IV. Cost and Performance

The system price was estimated by including the cost of all components an assembly charge and a generic markup of 2.4x (for distribution, profit, and selling costs). The computer program was used to optimize cost and performance assuming an increase in COP of 0.1 for the 22,000 BtuH size was worth \$600 (by reducing collector size). Table 3 shows the proportion of the system price and the amount attributable to the major components.

The system performance is described by the Coefficient of Performance (COP), and the system output of heat and of cooling. The systems are designed to a "design point". The heating design point and cooling design point use the ARI standards for indoor conditions (68°F indoors in winter and 78°F indoors in summer). In addition, the ARI summer outdoor design temperature is 95°F and the winter outdoor design point is 47°F. The output at 17°F is also used by the ARI. The HYCSOS was designed to a varying set of outdoor winter design temperatures.

Table 4 gives the system performance at the heating and cooling design temperatures. COP both including the electrical draw and excluding it are given.

Table 2. : Results of Design Optimization

WINTER DESIGN TEMP (°F)	HIGH TEMPERATURE BED COMPOSITION	EQUIVALENT FOAM DENSITY (lb)	FIN THICKNESS (INCHES)	FOAM DENSITY (lb)	BED DEPTH (INCHES)		ABSORPTION-DESORPTION TIME (MINUTES)	REGENERATION TIME (MINUTES)	SOLAR INPUT		OUTDOOR AIR TEMPERATURE CHANGE (°F)	HYDRIDE BED DESIGN HEAT TRANSFER RATE (BTU/H FT ²)
					HTD	LTD			WINTER	SUMMER		
25	LaNi ₄ 575 Al 425	35	.020	6.7	.231	.175	1	.16	256	278	5	6300
30	LaNi ₄ 459 Al 41	35	.020	6.7	.262	.201	1	.16	254	277	5	7200
25	LaNi ₄ 595 Al 405	35	.021	4.9	.325	.250	1	.16	257	280	5	8950
40	LaNi ₄ 605 Al 395	35	.021	4.9	.362	.281	1	.16	258	280	5	10050
45	Ca Ni ₅	35	.020	8.7	.236	.159	1	.16	211	224	3	5700
47	CaNi ₅	35	.021	4.8	.333	.224	1.5	.20	212	229	4	5350

Table 3. HYCSOS Component Price Breakdown and Total Price

WATER DESIGN TEMPERATURE (°F)	WATER OUT (°F)	WATER IN (°F)	FEED & RELEASE (°F)	INDOOR IN & FAN (°F)	INDOOR OUT & FAN (°F)	EXPANDED ALUMINUM TUBE (°F)	UNINSTALLED STEEL TOTAL PRICE
100	104	210.12	210.12	70.21	70.44	26.82	1728
	107	210.57	210.57	69.21	69.43	27.82	1745
	114	212.93	212.93	66.41	65.57	32.82	1758
114	104	201.05	201.05	72.25	72.44	26.82	1721
	107	201.72	201.72	72.21	72.47	27.82	1738
	120	212.63	212.63	66.44	65.53	32.82	1768
120	104	201.05	201.05	70.21	70.44	26.82	1707
	107	201.72	201.72	69.21	69.43	27.82	1724
	114	212.63	212.63	66.44	65.53	32.82	1769
130	104	201.05	201.05	70.21	70.44	26.82	1707
	107	201.72	201.72	69.21	69.43	27.82	1724
	120	212.63	212.63	66.44	65.53	32.82	1769
130	104	201.05	201.05	70.21	70.44	26.82	1707
	107	201.72	201.72	69.21	69.43	27.82	1724
	130	212.63	212.63	66.44	65.53	32.82	1769
140	104	201.05	201.05	70.21	70.44	26.82	1707
	107	201.72	201.72	69.21	69.43	27.82	1724
	130	212.63	212.63	66.44	65.53	32.82	1769
140	104	201.05	201.05	70.21	70.44	26.82	1707
	107	201.72	201.72	69.21	69.43	27.82	1724
	140	212.63	212.63	66.44	65.53	32.82	1769
150	104	201.05	201.05	70.21	70.44	26.82	1707
	107	201.72	201.72	69.21	69.43	27.82	1724
	150	212.63	212.63	66.44	65.53	32.82	1769
160	104	201.05	201.05	70.21	70.44	26.82	1707
	107	201.72	201.72	69.21	69.43	27.82	1724
	160	212.63	212.63	66.44	65.53	32.82	1769

Table 4. HYCSOS Design Point Performance

SOLAR INPUT WATERSIDE TEMPERATURE (°F)	SOLAR INPUT WATERSIDE TEMPERATURE (°F)		CHARACTERISTICS OF PERFORMANCE		ELECTRICAL OUTPUT (W)		HEAT OUTPUT SOLAR INPUT WATERSIDE TEMPERATURE (°F)	
	WATER OUT (°F)		WATER IN (°F)		ELECTRICAL OUTPUT (W)			
	WATER OUT (°F)	WATER IN (°F)	WATER OUT (°F)	WATER IN (°F)	PEAK	NET AVG		
100	104	210.12	210.12	70.21	80	42	1728	
	107	210.57	210.57	69.21	72	1.00		
	114	212.93	212.93	66.41	42	1.00		
114	104	201.05	201.05	72.25	120	42	1721	
	107	201.72	201.72	72.21	112	42		
	120	212.63	212.63	66.44	112	42		
120	104	201.05	201.05	70.21	80	42	1707	
	107	201.72	201.72	69.21	72	1.00		
	130	212.63	212.63	66.44	42	1.00		
130	104	201.05	201.05	70.21	80	42	1707	
	107	201.72	201.72	69.21	72	1.00		
	130	212.63	212.63	66.44	42	1.00		
140	104	201.05	201.05	70.21	80	42	1707	
	107	201.72	201.72	69.21	72	1.00		
	140	212.63	212.63	66.44	42	1.00		
150	104	201.05	201.05	70.21	80	42	1707	
	107	201.72	201.72	69.21	72	1.00		
	150	212.63	212.63	66.44	42	1.00		
160	104	201.05	201.05	70.21	80	42	1707	
	107	201.72	201.72	69.21	72	1.00		
	160	212.63	212.63	66.44	42	1.00		

The electrical output while heating is less than the electrical output while rejecting the heat outdoors because the power requirements for the indoor fan is higher than the outdoor fan. The use of a lower indoor fan speed would result in a somewhat higher net average power during power generation with indoor heating.

The performance of the HYCSOS at conditions which are more severe and milder than those at the design point is important for determining the seasonal performance and ultimately the cost effectiveness. Figures 11 and 12 show the heating and cooling output for temperatures other than at the design temperatures.

A solar absorption cooling system to provide 3 tons of cooling currently retails for \$3000 excluding a cooling tower, which is expensive, and an indoor heat exchanger. The HYCSOS system to provide 3 tons of cooling would cost \$3700 to \$3800, including all heat exchangers. HYCSOS also provides heating with a COP greater than one and electrical power, although it requires a higher solar input than the absorption unit (250° to 280°F as compared with 180°F), and has slightly lower cooling COPs. Thus this HYCSOS systems, which can be packaged similar to a conventional heat pump, compares favorably with a solar absorption cooling/direct solar heating unit.

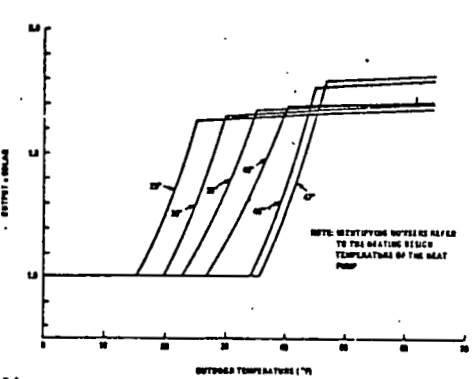


Fig. 11. Heating Output Relative to Design Point Solar Input

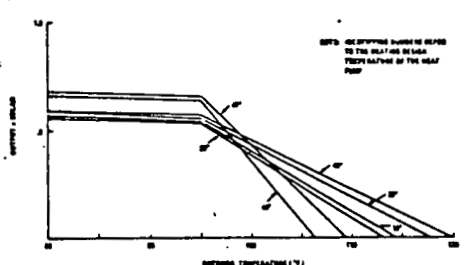


Fig. 12. Cooling Output Relative to Design Point Solar Input

References

1. "Hydride Heat Pump System for Building Air Conditioning Using High Temperature Solar Input" by Gorman, R. and Akridge, W. L., paper presented at the Concentrating Collection Workshop, September 26-28, 1977, Georgia Tech.
2. "The Affect of Aluminum Additions on the Thermodynamic and Structural Properties of LaNi₅-Al Hydrides," Mendelsohn, M. H., Gruen, D. M., and Dwight, A. E., Argonne National Laboratory.
3. "Duocel - A New Basic Design Material" Manufacturer's Literature from Energy Research and Generation, Inc., Oakland, California.
4. "Hydride Heat Pump," Volumes I and II, by Gorman, R., and Moritz, P., TRW Energy Systems Planning Division, McLean, Virginia, May 12, 1978.

METAL HYDRIDE SOLAR HEAT PUMP AND POWER SYSTEM (HYCSOS)

Dr. Richard Gorman, P.E., and
Ms. Pamela S. Moritz
TRW Energy Systems Division
7600 Colshire Drive
McLean, Virginia 22101

Abstract

This report presents the design, performance and cost of a solar-powered metal hydride heat pump and power system for use on a residence. This system was first conceived of and its feasibility demonstrated by Dieter Gruen, et. al., at Argonne National Laboratory. The system design, which is limited by heat transfer, was optimized via an iterative computer program. The design process starts with optimizing the thermal transport properties of the hydride-bed-heat exchanger, then traces temperatures and pressures through the operating cycles. The coefficient of performance (COP) of the overall system is then determined from the thermal losses due to cycling the hydride beds and due to the auxiliary power consumed by freon pumps and air-moving fans. The system, using high temperature solar collector input at 210°F to 280°F, provides heating with a COP of approximately 1.6 and cooling with a COP of approximately 0.6, and electrical power during spring and fall, all for a cost comparable to a solar absorption cooler.

I. Introduction

The use of solar energy for building heating and cooling has been a target for the past decade. The available technology (absorption and rankine cycle powered vapor compression refrigeration) have had low coefficients of performance (COP), and thus large solar collector sizes. These large solar collectors are then inactive for most of the spring and fall when heating and cooling are not needed.

The Hydride Conversion and Storage System (HYCSOS) provides heating, cooling and electrical power from solar energy or other low quality input heat. It would thus provide electrical, heat, and air-conditioning output from the solar collectors on a year-round basis. The cost for a HYCSOS which can do all these functions is the same or less than for a solar driven absorption unit of the same cooling capacity.

This investigation's aims are: designing a residential HYCSOS system, evaluating the performance of that design, and establishing the cost of that design. Previous investigations have established HYCSOS feasibility in the 100 ton size.

II. Theoretical Operation

The property of metal hydrides that is utilized for heat pump operation is that, at a given temperature and near constant pressures, metal alloys such as $\text{LaNi}_5\text{-Al}_3$ and CaNi_5 absorb hydrogen with the release of substantial amounts of heat. With heat input the process is reversible.

Figure 1² shows the characteristic pressure composition curve for $\text{LaNi}_{4.6}\text{-Al}_{0.4}$ at different temperatures. The use of the two dissimilar metal alloy systems which possess different hydriding isotherms enables one to pump heat from a lower to an intermediate temperature with heat supplied from a higher temperature.

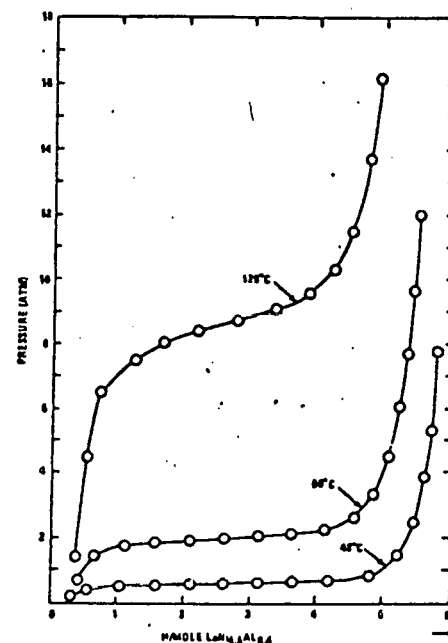


Fig. 1. Dissociation Pressure of $\text{LaNi}_{4.6}\text{-Al}_{0.4}\text{H}_n$

In its simplest form a hydride heat pump would consist of two hydride beds (each containing a different hydride) interconnected to allow hydrogen gas to flow between them. Means would be provided for the input of high temperature heat (from solar concentrating collectors); for heat rejection to or heat acquisition from the atmosphere; and for heat input to or heat rejection from the building. The heat pumping action of the system involves a four-step process. Figures 2 and 3 illustrate the theoretical process which is described below.

In the first step of the process, high temperature (solar) heat is applied to the first bed causing it to desorb hydrogen at high pressure. Because of the pressure differential between the beds, the hydrogen flows to the second bed which is at an intermediate temperature. The hydrogen is absorbed by the second bed with a release of